

# Geometric quantum gates robust against stochastic control errors

Shi-Liang Zhu<sup>1,2</sup> and Paolo Zanardi<sup>1</sup>

<sup>1</sup>*Institute for Scientific Interchange Foundation, Viale Settimio Severo 65, I-10133 Torino, Italy*

<sup>2</sup>*School of Physics and Telecommunication Engineering,  
South China Normal University, Guangzhou, China*

We analyze a scheme for quantum computation where quantum gates can be continuously changed from standard dynamic gates to purely geometric ones. These gates are enacted by controlling a set of parameters that are subject to unwanted stochastic fluctuations. This kind of noise results in a departure from the ideal case that can be quantified by a gate fidelity. We find that the maximum of this fidelity corresponds to quantum gates with a vanishing dynamical phase.

PACS numbers: 03.67.Lx, 03.65.Vf, 03.67.Pp

An essential prerequisite for quantum computation is the ability of maintaining quantum coherence and quantum entanglement in a information-processing system [1]. Unfortunately, since both these properties are very fragile against control errors as well as against unwanted couplings with environment, this goal is extremely hard to achieve. To this end several strategies have been developed, most notably: quantum error correction[2], decoherence-free subspace[3], and bang-bang techniques[4].

Quantum computation implemented by geometric phases[5, 6, 7] is believed to be another approach which can be used to overcome certain kinds of errors [8, 9, 10, 11, 12, 13, 14, 15]. It has been shown a universal set of quantum gates can be realized by geometric phases. However, the statement that quantum gates achieved by this way may have built-in fault-tolerant features (due to the fact that geometric phases depend only on some global geometric properties) has still the status of a conjecture and it has been the subject of some debate in the literature. Indeed this alleged resilience against errors of geometrical gates has been doubted by some numerical calculations with certain decohering mechanisms[16, 17]. On the other hand, analytical results show that adiabatic Berry's phase itself may be robust against dephasing[18] and stochastic fluctuations of control parameters [19]. These latter provide a sort of indirect evidence of the robustness of adiabatic geometric quantum computation; a more direct evidence would be given by a comparison between the fidelity of geometric gates and standard dynamic gates in presence of an error source. So far, this kind of convincing evidence, clearly showing that geometric quantum computation is robust against some realistic noise sources, is still missing.

In this paper we shall consider a parametric family of quantum gates subject to stochastic fluctuations of the control parameters. The departure from the ideal (i.e., no-fluctuation) case can be quantified by gate fidelity. We compute such a fidelity in a model where quantum gates can continuously change from standard dynamic gates to purely geometric ones. We find that *the maximum of fidelity corresponds to those cases in which the dynamical phase accumulated over the gate operation is zero*.

This provides a clear evidence of the robustness of nonadiabatic geometric computation in this specific scheme. The predictions presented here may be experimentally tested in some quantum computer prototypes. Moreover, this robustness of nonadiabatic geometric computation is relevant to experiments on quantum information processing; indeed it is generally believed that the control parameter nonuniformity is one of the most dangerous sources of errors for qubits in solid-state systems [20], NMR [21] and trapped ions [22], etc..

*Quantum computation via a pair of orthogonal cyclic states*– For universal quantum computation, it is sufficient to enact two of noncommuting single-qubit gates and one nontrivial two-qubit gate. Before to study the fidelity of a quantum gate subject to noise, we recall a scheme to implement a universal set of quantum gates by using a pair of orthogonal cyclic states[12, 13]. A single qubit gate given by

$$U^{(1)} = \begin{pmatrix} e^{i\gamma} \cos^2 \frac{\chi}{2} + e^{-i\gamma} \sin^2 \frac{\chi}{2} & i \sin \chi \sin \gamma \\ i \sin \chi \sin \gamma & e^{i\gamma} \sin^2 \frac{\chi}{2} + e^{-i\gamma} \cos^2 \frac{\chi}{2} \end{pmatrix}$$

can be obtained when a pair of cyclic states  $|\pm\rangle$  can be found for a unitary operation  $U^{(1)}$ , i.e.,  $U^{(1)}|\pm\rangle = e^{\pm i\gamma}|\pm\rangle$ . Here  $\chi$  is related to the initial cyclic states, and  $\gamma$  is a phase accumulated in the gate evolution. Usually the total phase  $\gamma$  consists of both geometric ( $\gamma_g$ ) and dynamic components ( $\gamma_d$ ), and  $U$  is specified as a geometric gate if  $\gamma$  is a pure geometric phase. Moreover, a conditional two-qubit gate can also be implemented if there exist, conditional to the state of control qubit, two different pairs of cyclic states of the target qubit. In terms of the computational basis  $\{|00\rangle, |01\rangle, |10\rangle, |11\rangle\}$ , where the first (second) bit represent the state of the control (target) qubit. The unitary operator describing the conditional two-qubit gate is given by  $U^{(2)} = \text{diag}(U_{(\gamma^0, \chi^0)}, U_{(\gamma^1, \chi^1)})$ , under the condition that the control qubit is off resonance in the manipulation of the target qubit. Here  $\gamma^\delta$  ( $\chi^\delta$ ) represents the total phase (the cyclic initial state) of the target qubit when the control qubit is in the state  $\delta (= 0, 1)$ . This scheme can be implemented in several realistic physical systems[12, 13].

*Control parameter fluctuation*– A simple approach for implementing  $U^{(1)}$  and  $U^{(2)}$  is to use an effective rotating

magnetic field to manipulate the state of qubits. In this case, the Hamiltonian for single qubit reads

$$H = (\omega_0\sigma_x \cos \omega t + \omega_0\sigma_y \sin \omega t + \omega_1\sigma_z)/2, \quad (1)$$

where  $\omega_i = -g\mu B_i/\hbar$  ( $i = 0, 1$ ) with  $g$  ( $\mu$ ) being the gyromagnetic ratio (Bohr magneton), and  $B_i$  ( $i = 1, 2$ ) acts as an external controllable parameter, and its magnitude can be experimentally changed. We also use this Hamiltonian to manipulate the target qubit in the implementation of two qubit gate when the control qubit is off resonance. The Hamiltonian of the two-qubit system is given by the Hamiltonian (1) plus the coupling Hamiltonian acting on the two qubits. In the non-ideal case the control fields contain randomly fluctuating components, here we assume that  $\omega_i$  is flatly distributed in the interval  $[(1 - \delta_i)\omega_i, (1 + \delta_i)\omega_i]$  with  $\delta_i$  a constant, and then we numerically calculate the average fidelity of quantum gates  $U^{(1)}$  and  $U^{(2)}$ . But we will assume that  $\omega$  is not affected by random fluctuations; this seems reasonable since frequency may be well controlled in a realistic experiment.

The average fidelity of a quantum gate we study is defined by

$$\overline{F} = \lim_{N \rightarrow \infty} \frac{1}{N} \sum_{j=1}^N \overline{F_j} = \lim_{N \rightarrow \infty} \frac{1}{N} \sum_{j=1}^N \overline{\left| \langle \psi_j^{in} | \hat{U}_{id}^\dagger | \psi_j^{out} \rangle \right|^2}, \quad (2)$$

where  $|\psi_j^{in}\rangle = [\cos \frac{\theta_j}{2} e^{-i\varphi_j/2}, \sin \frac{\theta_j}{2} e^{i\varphi_j/2}]^T$  or  $|\psi_j^{in}\rangle = [-\sin \frac{\theta_j}{2} e^{-i\varphi_j/2}, \cos \frac{\theta_j}{2} e^{i\varphi_j/2}]^T$  ( $T$  denotes the matrix transposition) is an input state.  $\theta_j \in [0, \pi]$  and  $\varphi_j \in [0, 2\pi]$  are randomly chosen in our numerical calculation.  $U_{id}$  is the ideal quantum gate without any control parameter fluctuation and  $|\psi_j^{out}\rangle$  is the output state after a noisy gate operation when the input state is  $|\psi_j^{in}\rangle$ . In the numerical calculation, we randomly choose one input state  $|\psi_j^{in}\rangle$ , and then calculate the average fidelity of  $\overline{F}_j$ , up to satisfactory convergence, for  $M$  configurations of fluctuations of magnetic fields. After that, we randomly choose the next input state and repeat the above calculation until deriving the fidelity of this specific input state with satisfactory convergence. We repeat  $N$  times to calculate the average fidelity by randomly choosing  $|\psi_j^{in}\rangle$ . In our numerical calculations below, we get small statistical errors when  $M$  and  $N$  are about several hundreds to one thousand.

*Fidelity of single-qubit gates*— The Schrödinger equation with Hamiltonian (1) can be analytically solved, and single qubit gates  $U^{(1)}$  can be achieved, where  $\chi = \arctan[\omega_0/(\omega_1 - \omega)]$  is the angle between the initial state and the symmetric axis of the rotating field. The corresponding phases for one cycle are given by  $\gamma_d = -\pi[\omega_0^2 + \omega_1(\omega_1 - \omega)]/\omega\Omega$ ,  $\gamma_g = -\pi[1 - (\omega_1 - \omega)/\Omega]$ , and  $\gamma = -\pi(1 + \Omega/\omega)$  with  $\Omega = \sqrt{\omega_0^2 + (\omega_1 - \omega)^2}$ . We can choose any two processes with different values  $\{\omega^j, \omega_0^j, \omega_1^j\}$  ( $j = 1, 2$ ) satisfying the constrain  $\sin \gamma_1 \sin \gamma_2 \sin(\chi_2 - \chi_1) \neq 0$  to enact two noncommuting single-qubit gates[13].

What is remarkable here is that quantum gate  $U^{(1)}$  implemented in this way can be varied continuously from a standard dynamic gate to a pure geometric gate, by changing the external parameters  $\{\omega, \omega_0, \omega_1\}$ . Hence, this scheme looks like an ideal model to compare the difference between geometric quantum gates and standard dynamic gates. It is straightforward to verify from the expression of  $\gamma_d$  that the dynamic phase is zero under the condition  $\omega = (\omega_0^2 + \omega_1^2)/\omega_1$ . Thus we can obtain purely geometric gates by choosing these specific parameters, such that  $\gamma_d = 0$  in the whole process. It has been shown that  $\chi$  in  $U^{(1)}$  can be controlled independently by the symmetric axis of the rotating field, and a specific quantum gate can be realized by a fixed phase  $\gamma$ . For example, the Hadamard gate is obtained by  $\gamma = (n_1 + 1/2)\pi$  and  $\chi = (n_2 + 1/4)\pi$  (with  $n_{1,2}$  integers). Therefore, we assume the total phase is fixed, for concreteness, we choose  $\gamma = -\beta\pi$  with  $\beta$  a constant. It is straightforward to check that  $\omega = (\omega_1 \pm \sqrt{\omega_1^2 - \eta(\omega_0^2 + \omega_1^2)})/\eta$  with  $\eta = 2\beta - \beta^2$  guarantee  $\gamma = -\beta\pi$ . The obvious requirement of  $\omega$  reality implies  $\eta\omega_0^2 \leq (1 - \eta)\omega_1^2$ . On the other hand, the dynamic phase is zero under the condition

$$\omega_1 = \omega_0 \sqrt{\eta/(1 - \eta)}. \quad (3)$$

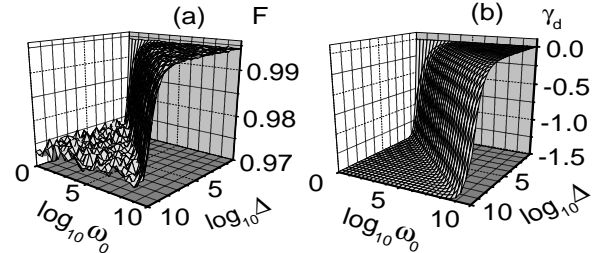


FIG. 1: The fidelity and phase in single qubit gates. (a) Fidelity, (b) dynamic phase.

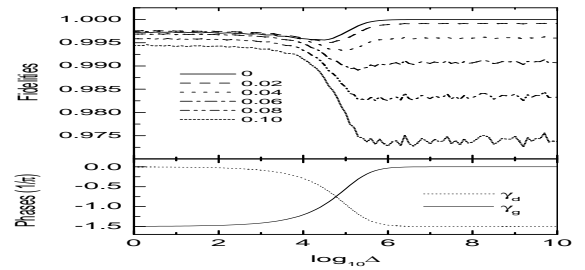


FIG. 2: The fidelities and phases in single qubit gate for  $\delta_0 = 0.1$ . The values of  $\delta_1$  are indicated. (a) Fidelities, (b) dynamic and geometric phases.

The fidelity  $F(\omega_0, \Delta)$  and dynamic phase of this gate for typical parameters are shown in Fig.1. Here  $\Delta$  is defined by  $\omega_1 = \sqrt{\eta/(1 - \eta)}\omega_0 + \Delta$ .  $\beta = 3/2$  is chosen just

as an example; we have checked that the main features described here are independent on this parameter. We plot  $F(\omega_0, \Delta)$  instead of  $F(\omega_0, \omega_1)$  to guarantee that  $\omega$  ( $= 2(2\omega_1 - \sqrt{\omega_1^2 - 3\omega_0^2})/3$ ) is a real number in the whole region. We can see several remarkable features from Fig.1, where  $\delta_0 = \delta_1 = 0.1$ : (i) the maximum of fidelity is along the line described by  $\Delta = 0$ , where the dynamic phase is zero; (ii) Fidelity is monotonically decreasing by increasing  $\Delta$ . The change of fidelity is slow at small  $\Delta$ , but very sharp near  $\Delta \sim \omega_0$ , and it is also slow for large values of  $\Delta$ . Remarkably, the changes of the absolute value of dynamic phases with  $\Delta$  are just as the same as the changes of the average fidelity of gates. Therefore, it clearly shows the close relation between the fidelity of quantum gates and the component of the dynamic (geometric) phase. This feature will be demonstrated also in the two-qubit case addressed later. We also checked the fidelity for different  $\delta_0$  and  $\delta_1$ . The fidelity and quantum phases as a function of  $\Delta$  for  $\omega_0 = 10^5$  are shown in Fig.2. We observe that the two main features discussed above appear, for the case  $\delta_0 = 0.1$ , when  $\delta_1$  is greater than 0.04. However, when  $\delta_1$  is less than 0.04, it is worth pointing out that the fidelity in the points with  $\Delta = 0$  is a local maximum, since there is a dip clearly shown nearby  $\Delta \sim \omega_0$ ; the largest fidelity appears when dynamic phase is dominant. We also numerically computed the fidelity for fixed  $\delta_1$  but varied  $\delta_0$  (not shown), the main features for different  $\delta_0$  are totally similar to those in Fig.1. The fact that the fidelity is larger when  $\Delta$  ( $\omega_1$ ) is large but with small fluctuation of  $\omega_1$  can be qualitatively explained from the dynamic phase  $\gamma_d$ . The deviation of  $\gamma_d$  from the noiseless case is dominated by the fluctuations of  $\omega_1$  when  $\Delta$  is much larger than  $\omega_0$ . Therefore the infidelity should be small if the fluctuations of  $\omega_1$  are very small.

*Fidelity of two-qubit gates*— We now numerically compute the fidelity of a two-qubit gate. We assume that the qubit-qubit interaction is given by  $H_I = J\sigma_z^{(1)}\sigma_z^{(2)}/2$ . This kind of coupling between qubits can be naturally realized, e.g., in quantum computer models with NMR and superconducting charge qubits coupled through capacitors. When the target qubit is manipulated by a rotating field described by Eq.(1) and control qubit is off resonance, it is shown that a two-qubit gate  $U^{(2)}$  with  $\chi^\delta = \arctan[\omega_0/(\omega_1^\delta - \omega)]$  and  $\gamma^\delta = -\pi(1 + \Omega^\delta/\omega)$  can be implemented. Here  $\omega_1^\delta = \omega_1 + (2\delta - 1)J$  and  $\Omega^\delta = \sqrt{\omega_0^2 + (\omega_1^\delta - \omega)^2}$ ,  $\omega$ ,  $\omega_0$ , and  $\omega_1$  are parameters for the target qubit. The corresponding phases for one cycle are given by  $\gamma_d^\delta = -\pi[\omega_0^2 + \omega_1^\delta(\omega_1^\delta - \omega)]/\omega\Omega^\delta$ , and  $\gamma_g^\delta = -\pi[1 - (\omega_1^\delta - \omega)/\Omega^\delta]$ . Besides, it is easy to check from  $\gamma_d^\delta = 0$  that the geometric two-qubit gates are realized whenever  $\omega = 2\omega_1$ , and  $\omega_1^2 = \omega_0^2 + J^2$ [13].

There is a lot of freedom in choosing parameters to implement a geometric quantum gate in the present scheme. One possible choice is given by  $\omega = \omega_1 + \sqrt{1 + \alpha^2}\omega_0$  and  $J = \alpha\omega_0$ , thus the speed of the purely geometric gate is of the same order of that of the dynamic gate.

To see the relation between the fidelity and the quantum phase, we plot the fidelity and dynamic phase of gate  $U^{(2)}$  just when  $\delta = 0$  as a function of the external parameters  $\omega_0$  and  $\omega_1$  in Fig.3. In this case, the dynamic phases change sharply nearby the line described by  $\log_{10}\omega_1 = \log_{10}(\sqrt{1 + \alpha^2}\omega_0)$ , where dynamic phases are zero, since it is straightforward to find that under the condition

$$\omega_1 = \sqrt{1 + \alpha^2}\omega_0, \quad (4)$$

$\gamma_d^\delta$  is zero. We can see from Fig.3 that the maximum of fidelity is along the line where the dynamic phase is zero. Moreover, compared with the single-qubit case shown in Fig.1, the fidelity of the gate shown here decreases quickly, since the dynamic phase changes sharply when the parameters do not satisfy Eq.(4). Therefore, it is clearly shown the close relation between the change of fidelity and the change of dynamic component of the phase.

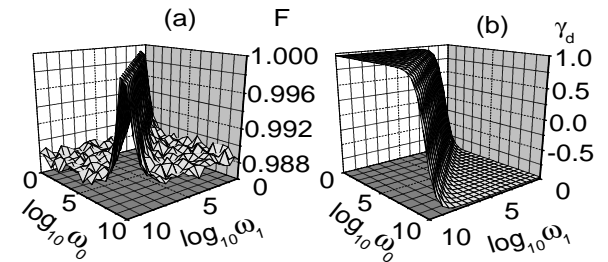


FIG. 3: The fidelity and phase in two-qubit gates for  $\delta_0 = \delta_1 = 0.1$ ,  $\delta = 0$  and  $\alpha = \sqrt{3}$ . (a) Fidelity, (b) dynamic phase.

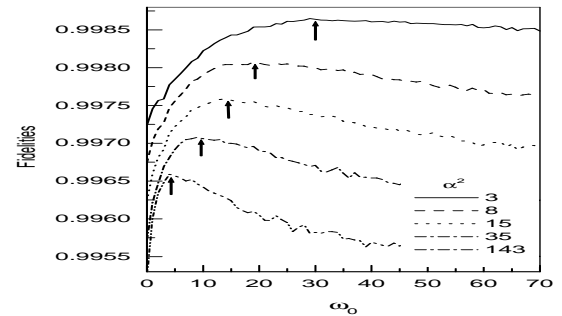


FIG. 4: The fidelities of two-qubit gates. The curves for different  $\alpha$  are vertically shifted for clarity. Points with zero dynamic phases shown in Eq.(4) are denoted by arrows.

To show in a more clear fashion that the maximum of fidelity is along the line described by Eq.(4) and that this feature is independent on the parameter  $\alpha$ , we numerically computed the average fidelity of  $U^{(2)}$  when the state of the control qubit is unfixed. The fidelity as a function of  $\omega_0$  for  $\omega_1 = 60$ ,  $\delta_0 = \delta_1 = 0.05$  and

$\alpha = \sqrt{3}, \sqrt{8}, \sqrt{15}, \sqrt{35}, \sqrt{143}$  are plotted in Fig.4. It is easy to derive from Eq.(4) that the dynamic phase is zero at  $\omega_0 = 30, 20, 15, 10, 5$ , and these points are denoted by arrows in Fig.4. We observe that the maxima of fidelity are indeed at the points described by Eq.(4), where the dynamic phases are zero; this property is independent on  $\alpha$ .

*Comparison with previous results*— We would like to compare the results here with the previous results in literature. It has been shown that the effects of fluctuations of the control parameters[17] or decoherence described by Lindblad form[16] on nonadiabatic gates are more severe than for the standard dynamic gates. We note that in Refs.[16, 17] the geometric gate is implemented by three rotations, but only one operation is used to realize a standard dynamic gate. Thus a direct comparison is somewhat not appropriate, and one can not rule out other possibilities. In the present model, however, the operations for both dynamic gate and geometric gate are totally the same, except that the controllable parameters vary continuously. In this sense this model looks definitely more suitable to assess the difference between geometric gates and dynamic gates as far as noise resilience is concerned.

Before concluding, we would like to point out that the scheme studied here is based on nonadiabatic operations. Note that  $\omega$  is of the same order of the magnitude as  $\omega_0$  or  $\omega_1$  in both one and two-qubit gate operations. This implies that the speed of geometric quantum gate here in-

vestigated is comparable with that of the dynamic quantum gate. In contrast, the speed of quantum gate based on adiabatic Berry's phase is much lower than that of gate using dynamic phase, since the adiabatic condition requires that both  $\omega_0$  and  $\omega_1$  should be much larger than  $\omega$ . Thus the speed constraint required by adiabatic geometric gates is removed in the present scheme, and the results discussed above show the robustness of this nonadiabatic geometric gates against noise in the control parameters. This considerations suggest that this approach to quantum computation should be significant in quantum information processing.

*Conclusions*— In this paper we have numerically computed the average fidelity of a family of quantum gates, which vary continuously from the standard dynamic gates to pure geometric gates with the change of experimentally controllable parameters. We found that the maximum of gate fidelity is achieved along the line where the dynamical phase is zero. We believe that the results presented in this paper provide a first convincing evidence of the robustness of geometric computation. Our predictions can be, in principle, experimentally tested in already existing quantum computer prototypes, such as NMR, trapped ions and superconducting qubits, etc..

This work was supported by the European Union project TOPQIP (contract IST-2001-39215). S.L.Z. was supported by the NSFC under Grant No.10204008 and the NSF of Guangdong under Grant No.021088.

---

[1] See e.g., D.P. DiVincenzo and C. Bennett, *Nature* **404**, 247 (2000)

[2] P. W. Shor, *Phys. Rev. A* **52**, R2493 (1995); A. M. Steane, *Phys. Rev. Lett.* **77**, 793 (1996).

[3] L. M. Duan and G. C. Guo, *Phys. Rev. Lett.* **79**, 1953 (1997); P. Zanardi and M. Rasetti, *ibid.* **79**, 3306 (1997).

[4] L. Viola and S. Lloyd, *Phys. Rev. A* **58**, 2733 (1998); P. Zanardi, *Phys. Lett. A* **258**, 77 (1999).

[5] M. V. Berry, *Proc. R. Soc. London* **A392**, 45 (1984).

[6] Y. Aharonov and J. Anandan, *Phys. Rev. Lett.* **58**, 1953 (1987).

[7] S. L. Zhu, Z. D. Wang, and Y. D. Zhang, *Phys. Rev. B* **61**, 114 (2000).

[8] P. Zanardi and M. Rasetti, *Phys. Lett. A* **264**, 94 (1999).

[9] J.A.Jones, V.Vedral, A.Ekert, and G.Castagnoli, *Nature (London)* **403**, 869 (2000).

[10] L.M.Duan, J.I.Cirac, and P.Zoller, *Science* **292**, 1695 (2001).

[11] X. B. Wang and M. Keiji, *Phys. Rev. Lett.* **87**, 097901 (2001).

[12] S.L.Zhu and Z.D.Wang, *Phys. Rev. Lett.* **89**, 097902 (2002); *Phys. Rev. A* **66**, 042322 (2002).

[13] S. L. Zhu and Z. D. Wang, *Phys. Rev. A* **67**, 022319 (2003).

[14] D.Leibfried, B.DeMarco, V.Meyer, D.Lucas, M.Barrett, J.Britton, W.M.Itano, B.Jelenkovic, C.Langer, T.Rosenband, and D.J.Wineland, *Nature (London)* **422**, 412 (2003); S. L. Zhu and Z. D. Wang, *Phys. Rev. Lett.* **91**, 187902 (2003).

[15] P. Solinas, P. Zanardi, and N. Zanghi, *quant-ph/0312109* (2003).

[16] A. Nazir, T. P. Spiller, and W. J. Munro, *Phys. Rev. A* **65**, 042303 (2002).

[17] A. Blais and A. -M. S. Tremblay, *Phys. Rev. A* **67**, 012308 (2003).

[18] A. Carollo, I. Fuentes-Guridi, M. F. Santos, and V. Vedral, *Phys. Rev. Lett.* **92**, 020402 (2004); *ibid.* **90**, 160402 (2003).

[19] G. D. Chiara and G. M. Palma, *Phys. Rev. Lett.* **91**, 090404 (2003).

[20] Y.Makhlin, G.Schön, and A.Shirman, *Rev. Mod. Phys.* **73**, 357 (2001).

[21] L. M. K. Vandersypen and I. L. Chuang, *quant-ph/0404064*.

[22] J. J. Garcia-Ripoll and J. I. Cirac, *Phys. Rev. Lett.* **90**, 127902 (2003).